J. Fluid Mech. (1971), *vol.* 49, *part* 4, *pp.* 693–703
Printed in Great Britain

Effect of a non-uniform alternating electric field on the thermal boundary layer near a heated vertical plate

By ROBERT J. TURNBULL

Department of Electrical Engineering, University of Illinois, Urbana, Illinois 61801

(Received 4 February 1971)

A thermal boundary layer is established by heating a vertical plate in a dielectric liquid. An alternating voltage is applied between the heated plate and another plate which is not parallel to the heated plate. This voltage produces a non-uniform electric field which in turn produces electrical forces acting on the gradients in dielectric permittivity which result from the temperature gradients. These electrical forces alter the boundary layer. In this paper approximate equations are developed which allow one to calculate the boundary-layer thickness, velocity, and Nusselt numbers for the boundary layer in the presence of the non-uniform electric field. Numerical calculations show that the heat-transfer coefficient can be either increased or decreased by the non-uniform field, depending on whether the field is strongest at the top or bottom of the plates and also on the field strength. Experiments were performed which demonstrate the change in heat transfer caused by the non-uniform field.

1. Introduction

The problem to be analyzed in the paper is shown in figure 1. A heated vertical plate is placed in a dielectric liquid, causing a thermal boundary layer to form next to the plate. A second plate is placed in the fluid such that the plates are not parallel. An alternating voltage is applied between the plates, producing a non-uniform electric field. The field may be largest at the bottom, as shown in figure 1 (*a*), or largest at the top as in figure 1 (*b*). The effect of the non-uniform field on the boundary layer is the subject of this paper. The frequency of the voltage is high enough so that no free charge is present in the fluid.

The electrical forces in the absence of free charge are the dielectrophoretic forces. (See equation (6).) The effective part of these forces is proportional to the electric field squared times the gradient in dielectric constant and is in the direction of decreasing dielectric constant. The effect of these forces is to tend to pull the liquid with highest dielectric constant into the strongest field. For a dielectric liquid the highest dielectric constant occurs at the lowest temperature. Thus, the coolest fluid tends to be pulled into the region of strongest field. If the region of strongest field is at the bottom the electric field effectively enhances gravity, increasing the heat-transfer coefficient. If the strongest field is at the top, it

would be expected that the effective gravity would be reduced and the heat-transfer coefficient decreased. As we will see later, at high field strengths other effects come into play.

Free convection caused by heating a vertical plate has been studied extensively. Ede (1967) contains a review of the work on this problem. Turnbull (1969, 1971) is concerned with the effects of d.c. electric fields on the thermal boundary layer near a heated vertical plate, the first paper treating the effect of

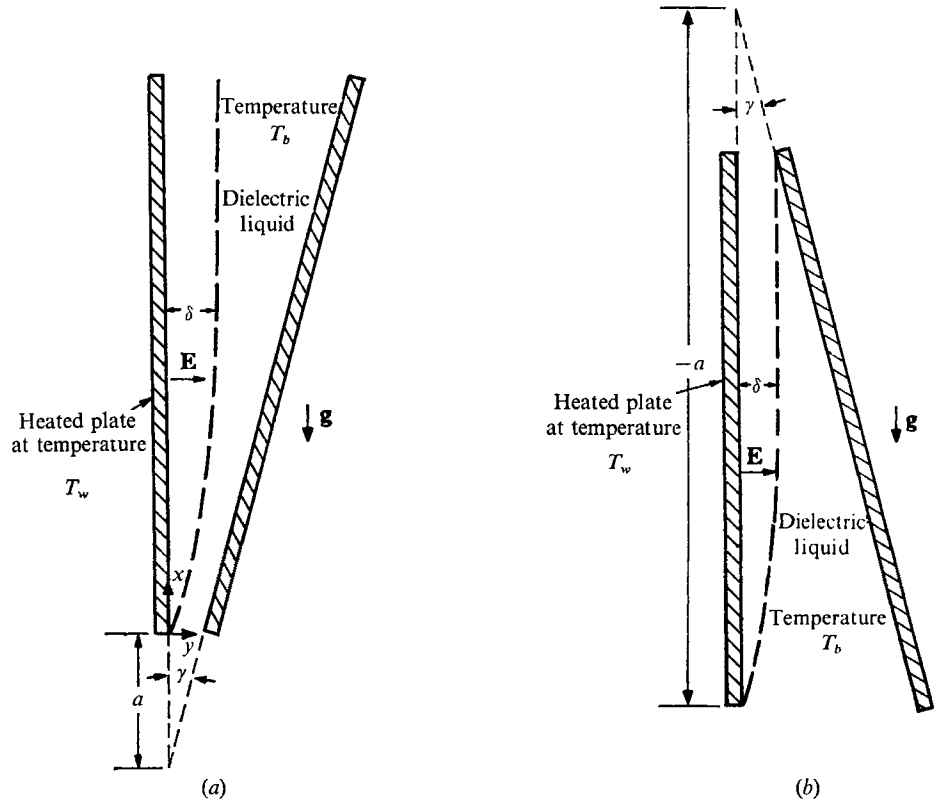

FIGURE 1. Configuration of thermal boundary layer and electric field. The electric field is imposed between the two non-parallel plates. (*a*) Field strongest at the bottom. (*b*) Field strongest at the top.

the field on a stable boundary layer, and the second the instability caused by the electric field. A survey of previous work on heat transfer in electric fields also appears in Turnbull (1969).

2. Theoretical analysis

In this section a set of approximate ordinary differential equations will be developed. These equations may be solved to find the boundary-layer thickness, fluid velocity and heat-transfer coefficient as functions of vertical position. The method used is similar to that of Squire (1938).

The mechanical equations governing the fluid motions are, if the fluid is assumed to be incompressible and the viscosity is constant,

$$\nabla . \mathbf{v} = 0, \tag{1}$$

$$\rho(D\mathbf{v}/Dt) = -\nabla p + \rho\mathbf{g} + \mathbf{f}_e + \mu\nabla^2\mathbf{v}, \tag{2}$$

where $\mathbf{v}$ is the velocity, ρ the density, $D/Dt = \partial/\partial t + \mathbf{v}.\nabla$, p is the pressure, $\mathbf{g}$ is the acceleration of gravity, $\mathbf{f}_e$ is the force due to the electric field and μ is the dynamic viscosity. The equation of heat conduction, neglecting the viscous heating, is

$$\rho c DT/Dt = \nabla . (k\nabla T), \tag{3}$$

where T is the temperature, c the specific heat, and k the thermal conductivity.

The electrical equations in the absence of free charge are

$$\nabla \times \mathbf{E} = 0, \tag{4}$$

$$\nabla . (\epsilon \mathbf{E}) = 0, \tag{5}$$

where E is the electric field and ϵ the dielectric permittivity. The condition for there to be no free charge is that the period of the alternating field be much less than the dielectric relaxation time, ϵ/σ, where σ is the electrical conductivity. The electrical force density under these conditions is (Stratton 1941)

$$\mathbf{f}_e = -\tfrac{1}{2}(\mathbf{E}.\mathbf{E})\nabla\epsilon + \tfrac{1}{2}\nabla\left(\mathbf{E}.\mathbf{E}\rho\frac{\partial\epsilon}{\partial\rho}\right). \tag{6}$$

To complete the equations necessary for describing the motions, the functional dependence of the fluid properties on temperature is needed. The density and permittivity are assumed linear functions of temperature and the thermal diffusivity, κ, is assumed independent of temperature.

$$\rho = \rho_b[1 - \beta(T - T_b)], \tag{7}$$

$$\epsilon = \epsilon_b[1 - \alpha(T - T_b)]. \tag{8}$$

T_b is the temperature of the bulk of the fluid and ρ_b and ϵ_b are the fluid properties there.

The electric field is non-uniform both because the plates are not parallel and because the permittivity is not constant. The dielectric permittivity varies on the order of 0·1 % per degree Centigrade in dielectric liquids. Therefore, the gradients in the field due to gradients in the permittivity are small and will be neglected compared to the field gradients due to the non-parallel plates. The resulting electric field distribution is

$$\text{vertical component} \quad E_x = \frac{-Vy}{\gamma[(x+a)^2 + y^2]},$$

$$\text{horizontal component} \quad E_y = \frac{V|x+a|}{\gamma[(x+a)^2 + y^2]}, \tag{9}$$

where V is the voltage between the plates, γ is the angle between the plates and a is the distance from the bottom of the heated plate to the line where the planes of the two plates intersect. a is positive if the plates are closer together at the bottom and negative if closer together at the top.

Since the motion is two-dimensional, (1) has two non-zero components which are

$$\rho\left(\frac{\partial u}{\partial t}+u\frac{\partial u}{\partial x}+v\frac{\partial u}{\partial y}\right)=-\frac{\partial p}{\partial x}-\rho g-\tfrac{1}{2}(E_x^2+E_y^2)\frac{\partial \epsilon}{\partial x}+\frac{1}{2}\frac{\partial}{\partial x}\left[(E_x^2+E_y^2)\rho\frac{\partial \epsilon}{\partial \rho}\right]+\mu\left(\frac{\partial^2 u}{\partial x^2}+\frac{\partial^2 u}{\partial y^2}\right), \quad (10)$$

$$\rho\left(\frac{\partial v}{\partial t}+u\frac{\partial v}{\partial x}+v\frac{\partial v}{\partial y}\right)=-\frac{\partial p}{\partial y}-\tfrac{1}{2}(E_x^2+E_y^2)\frac{\partial \epsilon}{\partial y}+\frac{1}{2}\frac{\partial}{\partial y}\left[(E_x^2+E_y^2)\rho\frac{\partial \epsilon}{\partial \rho}\right]+\mu\left(\frac{\partial^2 v}{\partial x^2}+\frac{\partial^2 v}{\partial y^2}\right). \quad (11)$$

In order to find the steady-state solution for the boundary layer, time derivatives are set to zero. Taking the partial derivative with respect to y of (10) and subtracting the partial derivative with respect to x of (11) yields, if non-uniformities in densities are neglected in the inertial terms,

$$\rho_b\left[-u\left(\frac{\partial^2 v}{\partial x^2}+\frac{\partial^2 v}{\partial y^2}\right)+v\left(\frac{\partial^2 u}{\partial x^2}+\frac{\partial^2 u}{\partial y^2}\right)\right]=-g\frac{\partial \rho}{\partial y}-\frac{1}{2}\frac{\partial}{\partial y}(E_x^2+E_y^2)\frac{\partial \epsilon}{\partial x}+\frac{1}{2}\frac{\partial}{\partial x}(E_x^2+E_y^2)\frac{\partial \epsilon}{\partial y}+\mu\left[\frac{\partial^3 u}{\partial x^2\partial y}+\frac{\partial^3 u}{\partial y^3}-\frac{\partial^3 v}{\partial x^3}-\frac{\partial^3 v}{\partial x\partial y^2}\right]. \quad (12)$$

Because the boundary layer is thin, approximations may be made in (12). First, the derivatives of the velocity components with respect to y are much larger than their derivatives with respect to x. Since the dielectric permittivity depends only on the temperature, $|\partial\epsilon/\partial y| \gg |\partial\epsilon/\partial x|$. If the boundary-layer thickness, δ, is much less than $|x+a|$, then $|\partial(E_x^2+E_y^2)/\partial x| \gg |\partial(E_x^2+E_y^2)/\partial y|$. Equation (12) now reduces to

$$\rho_b\left[-u\frac{\partial^2 v}{\partial y^2}+v\frac{\partial^2 u}{\partial y^2}\right]=-g\frac{\partial \rho}{\partial y}+\frac{1}{2}\frac{\partial(E_x^2+E_y^2)}{\partial x}\frac{\partial \epsilon}{\partial y}+\mu\frac{\partial^3 u}{\partial y^3}. \quad (13)$$

We also have

$$\frac{\partial(E_x^2+E_y^2)}{\partial x}=\frac{-2V^2}{\gamma^2(x+a)^3}. \quad (14)$$

Integrating (13) with respect to y gives

$$\rho_b\left[u\frac{\partial u}{\partial x}+v\frac{\partial u}{\partial y}\right]=-\rho g-\epsilon\frac{V^2}{\gamma^2(x+a)^3}+\mu\frac{\partial^2 u}{\partial y^2}+C(x), \quad (15)$$

where $C(x)$ is a constant of integration. Outside the boundary layer the velocity is zero and the temperature is T_b. Therefore,

$$C(x)=+\rho_b g+\epsilon_b\frac{V^2}{\gamma^2(x+a)^3} \quad (16)$$

and (15) is

$$\rho_b\left[u\frac{\partial u}{\partial x}+v\frac{\partial u}{\partial y}\right]=\rho_b g\beta(T-T_b)+\epsilon_b\alpha(T-T_b)\frac{V^2}{\gamma^2(x+a)^3}+\mu\frac{\partial^2 u}{\partial y^2}. \quad (17)$$

It can be seen from (17) that the electric field either adds to or subtracts from the force of gravity depending on the sign of $x+a$. When $x+a$ is positive, the field is largest at the bottom, the electrical forces add to the gravitational one, increasing the convection in the boundary layer. If the field is largest at the top, the electrical forces are opposite to the gravitational one, thus reducing the velocity in the boundary layer.

If we take the steady-state form of (3) and apply the boundary-layer approximation, the result is

$$u\frac{\partial T}{\partial x}+v\frac{\partial T}{\partial y}=\kappa\frac{\partial^2 T}{\partial y^2}. \tag{18}$$

Equations (17) and (18) may be solved to find the velocity and temperature distribution in the boundary layer. The solution to these equations will differ from the ordinary thermal boundary-layer solution since the electrical force depends on both T and on vertical position x, while the gravitational force in (17) depends on T only. In order to solve these equations, we will use the technique of Squire (1938). This involves assuming velocity and temperature profiles in the horizontal direction and integrating the equations from 0 to δ in y (from the plate to the edge of the boundary layer). The profiles which will be used are the same as in Squire (1938) for the ordinary boundary layer. The reason the same profiles were picked is that the electric field term and the gravitational term in (17) both have the same horizontal dependence for a given vertical position. Therefore, we assume

$$u = U(y/\delta)(1-y/\delta)^2, \tag{19}$$

$$T = T_b+(T_w-T_b)(1-y/\delta)^2, \tag{20}$$

where U and δ are functions of x.

If (19) and (20) are substituted into (17) and (18) and then (17) and (18) integrated over y from 0 to δ and the results non-dimensionalized, the following equations are obtained.

$$\frac{1}{105}\frac{d}{dx'}(U'^2\delta') = [1+F/(1+x'/a')^3](\delta'/3)-U'/\delta', \tag{21}$$

$$\frac{1}{30}\frac{d}{dx'}(\delta'U') = (2/Pr)(1/\delta'). \tag{22}$$

The primes denote dimensionless quantities. The length scale is

$$L = (\mu^2/\rho_b^2 g\beta(T_w-T_b))^{\frac{1}{3}} \tag{23}$$

and the time scale is

$$\tau = (\mu/\rho_b g^2\beta^2(T_w-T_b)^2)^{\frac{1}{3}}. \tag{24}$$

The other quantities appearing in (21) and (22) are defined as

$$U' = U\tau/L; \quad \delta' = \delta/L; \quad x' = x/L;$$

$$a' = a/L; \quad Pr = \mu/\rho_b\kappa; \quad F = (V^2\alpha\epsilon_b/\gamma^2 a^3\rho_b g\beta).$$

Pr is the Prandtl number and F is the ratio of the electrical forces to the gravitational forces at the bottom of the plate. Equations (21) and (22) are ordinary non-linear differential equations which may be solved by numerical techniques. Numerical solutions of these equations will be considered in the next section.

3. Numerical results

In order to determine the effect of the electric field on the boundary layer, (21) and (22) were solved numerically. The conditions for which the numerical solutions were obtained were a Prandtl number of 100, a dimensionless plate height of 50 with the plates of the two electrodes intersecting at a dimensionless

distance of ten from the end of the plates. Calculations were made both for the electrodes closest together at the bottom and for the electrodes closest together at the top. Several different values of the voltage were tried for each case. The results of the numerical calculations are shown in figures 2–4. To facilitate comparison between the case with the plates closer at the top and the case with the plates closer at the bottom, a new parameter F' will be defined:

$$F' = \begin{cases} F & (F > 0), \\ F\left(\dfrac{a'}{h'+a'}\right)^3 & (F < 0), \end{cases} \tag{25}$$

where h' is the dimensionless height of the plate. F' is the ratio of electrical forces to gravitational forces at the end where the plates are closest. F is the same ratio

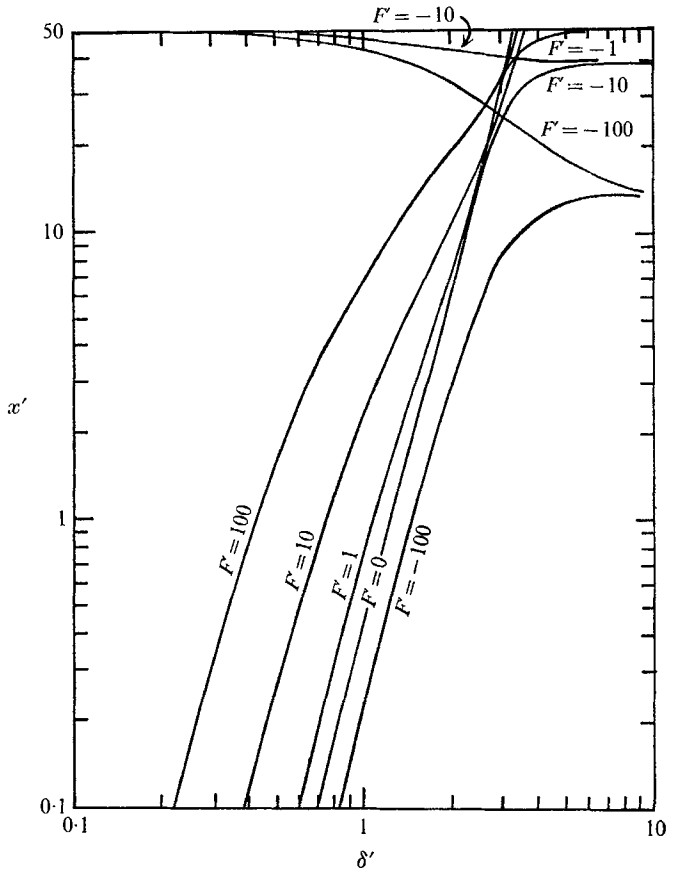

FIGURE 2. Dimensionless boundary-layer thickness as a function of position for various voltages. For this figure $Pr = 100$, the dimensionless plate height is 50 and the point where the planes of the two plates intersect is a dimensionless distance ten from the end of the plate.

at the lower end of the plates. If the apparatus is turned upside down and the same voltage is applied, the magnitude of F' remains the same. (The sign is changed, however.)

Figure 2 contains plots of the boundary-layer thickness, δ', versus position in

the vertical direction, x', for various values of F'. $a' = 10$ when $F' > 0$ and $a' = -60$ when $F' < 0$. The case for $a' = -60$ is the same as for $a' = 10$ except the apparatus is turned upside down. For no voltage ($F' = 0$) the $\delta' - x'$ curve is a straight line on the log-log plot. This is the solution

$$\delta' = 3{\cdot}93\, Pr^{-\frac{1}{2}} (Pr + 20/21)^{\frac{1}{4}} x'^{\frac{1}{4}}$$

obtained by Squire (1938). When the plates are closer together at the bottom ($F' > 0$) the electric field forces tend to move the fluid in the same direction as the gravitational forces. For this case, the application of a voltage makes the boundary layer thinner. The difference in boundary-layer thickness when there is an applied voltage and when there is no voltage is greatest (in relative terms) at the bottom. The differences become smaller as x' (the vertical co-ordinate) is increased until the boundary layers are approximately the same thickness. This is to be expected since the electric field term in (21) decreases with increasing x'. The larger the voltage, the thinner the boundary layer and the higher the point on the plate where the electric field effects become negligible.

When the electrodes are closer together at the top ($F' < 0$), the electrical forces tend to move the fluid in the opposite direction from the gravitational forces. For $F' = -1$ the forces just cancel at the top of the heated plate; everywhere else the gravitational forces are larger. In this case the boundary-layer thickness differs from the no-voltage solution only near the top of the plate where it is larger. The solution for the boundary-layer thickness goes to infinity at the top edge of the plate. As the voltage is increased the point where the forces cancel moves down the heated plate. Below the cancellation point the boundary layer becomes thicker than it was with no voltage with the thickness going to infinity at the cancellation point. Of course, the solution was obtained using equations with boundary-layer approximations which are not valid in the vicinity of the cancellation point. Above the cancellation point, the net force near the plate is directed downward and a boundary layer is set up with the velocity also directed downward. The thickness of this boundary layer rises from zero at the top edge of the heated plate to infinity at the cancellation point.

Figure 3 shows the effect of the electric field on the velocity in the boundary layer, U'. For no voltages the solution is $U' = 5{\cdot}17\,(Pr + 20/21)^{-\frac{1}{2}} x'^{\frac{1}{2}}$. For $F' > 0$, increasing the voltage increases the velocity with the increase being greatest at the lower end of the plate. For negative F', increasing the voltage causes the velocity to decrease below the cancellation point. The velocity then goes to zero at the cancellation point. Above the cancellation point the velocity is directed downward ($U' < 0$) with the magnitude rising from zero at the top edge of the heated plate to a maximum and then decreasing to zero at the cancellation point.

The other quantity which was calculated numerically was the Nusselt number based on the height of the plate. The Nusselt number is defined as the power transferred across the boundary layer divided by the power which would be transferred purely by heat conduction across a fluid layer whose thickness equals the height of the plate and whose temperature difference is the same as for the boundary layer. The results of the Nusselt number calculations are shown in figure 4. The solution for no voltage is $Nu = 40{\cdot}19$. For $F' > 0$ increasing the

voltage results in an increased Nusselt number because of the decrease in the boundary-layer thickness. For $F' < 0$, increasing the voltage results in a decreasing Nusselt number until F' reaches minus one. Further increases in the voltage result in an increasing Nusselt number. The explanation is as follows. For $0 > F' > -1$ the electric field increases the boundary-layer thickness. For $F' < -1$ there exist two boundary layers. The one below the cancellation point is thicker than in the zero voltage case and therefore transfers less heat. However, the boundary layer above the cancellation point is thinner than the zero voltage boundary layer near the top of the plate. As the voltage is raised this upper boundary layer becomes thinner, thus increasing the heat transfer.

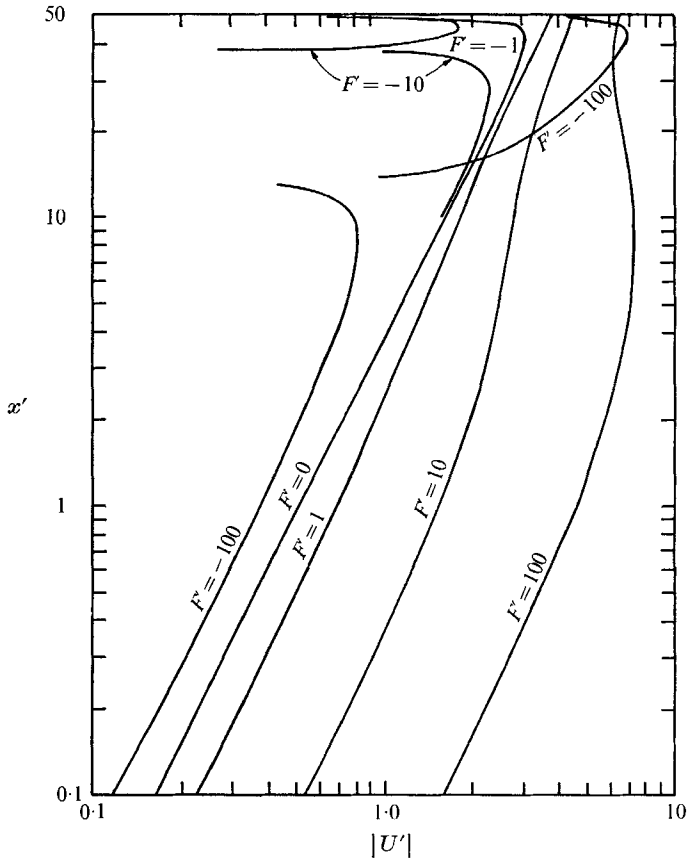

FIGURE 3. Dimensionless velocity in the boundary layer as a function of position. Same conditions as in figure 2.

4. Experimental results

In order to test the theoretical results of the previous sections, an experiment was performed. By measuring the temperatures of the two electrodes for various voltages, the dependence of the Nusselt number on voltage could be obtained. The experiments were done using fields which were strongest at the bottom.

The dimensions of the system were: plate height, 4·75 in., plate width, 3·5 in., and plate separation, 0·5 in. at the top and 0·1875 in. at the bottom.

The fluid used was Dow Corning 200 Fluid-100 Centistoke grade and the frequency of the voltage was 60 Hz. If an ohmic conductivity model is used, published data indicate a time constant for charge accumulation of about 10^3 sec for this liquid. Thus the frequency of the voltage seems high enough to prevent the accumulation of free charge. The results of another experiment (Turnbull 1970) using the same liquid and frequency were successfully predicted neglecting free charge. Application of the voltage resulted in increases in the Nusselt number as predicted by the numerical calculations. The results of the experiments are

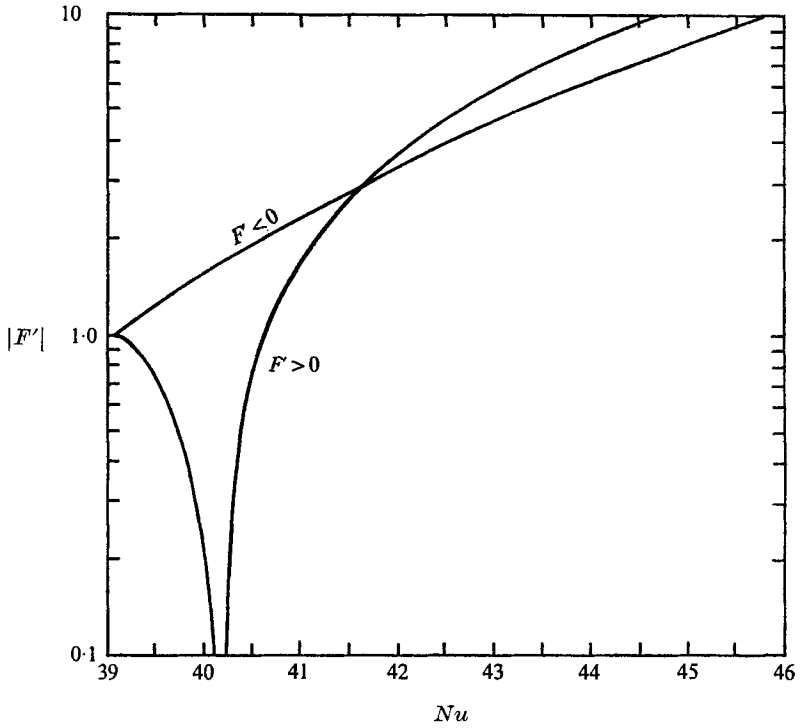

FIGURE 4. Nusselt number for various voltages. The other parameters are the same as in figure 2.

shown in figure 5. This graph was plotted as follows. On the horizontal axis is the ratio of the experimental Nusselt number with a voltage applied to the experimental Nusselt number with no voltage. The experimental value with no electric field was found by taking all the experimental points with no E-field and doing a least-squares fit of the equation $Nu = C_1 Ra^{\frac{1}{4}} + C_2$ where Ra is the Rayleigh number and C_1 and C_2 are found from the least-squares fit. This form of the equation was chosen since the approximate theory (Squire 1938) predicts a Nusselt number proportional to $Ra^{\frac{1}{4}}$. Most of the zero voltage points agree with this curve to within 2 % and all within four per cent. The vertical axis is the ratio of the theoretical Nusselt number (calculated from (21) and (22) using the experimental

data) to the theoretical Nusselt number calculated using the same data except assuming that the voltage was zero. It has been assumed that the power into the heated plate is divided equally between the two boundary layers on the sides of the plate.

It can be seen from figure 5 that the measured percentage increases in heat transfer due to the electric field are greater than those predicted by the theory. Each of the horizontal collections of points in figure 5 consists of data taken at a particular voltage. The lowest group is at 13·48 kV, the middle group at 17·75 kV and the highest group at 20·20 kV. The experiment was performed as follows. The heater and the voltage were turned on simultaneously. After the boundary layer was formed, the temperatures of the two electrodes were measured at regular time intervals. During this time the liquid and the plate were both rising in temperature thus giving data for a variety of Prandtl numbers. Of the data taken at each voltage, the points toward the left in figure 5 were taken when the liquid was coolest and those toward the right were taken when the liquid was warmest.

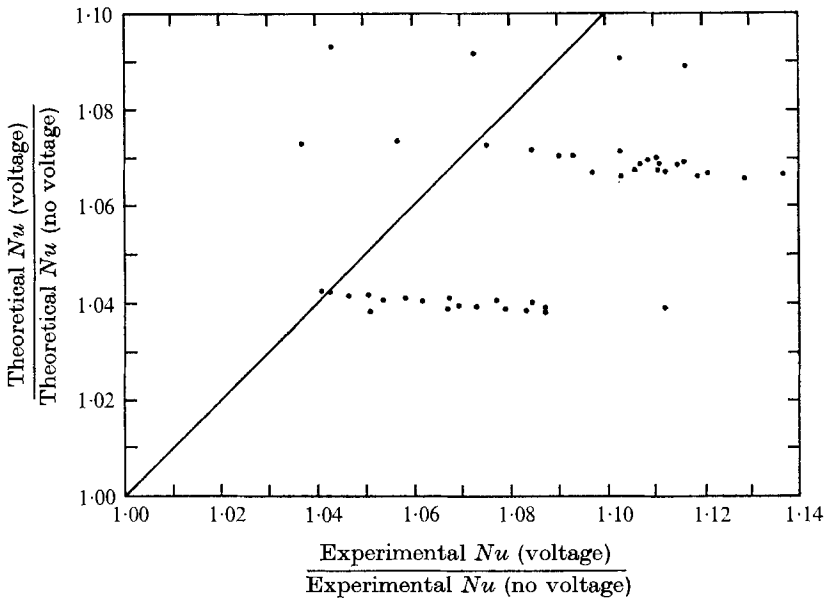

FIGURE 5. Comparison of experimental results with theoretical calculations. The horizontal axis is the ratio of the experimental Nusselt number with an electric field to that with no electric field. The vertical axis is the ratio of the theoretical Nusselt number with an electric field to that with no electric field.

To understand the reason for the scatter in the experimental data consider the following model. The power into the heated plate, which is held constant, divides up to flow through the two boundary layers on the sides of the plate. These boundary layers can be represented by thermal resistances. The liquid on each side of the plate is represented by a thermal capacity. The air surrounding the apparatus tends to cool it so on each side of the plate there is a thermal resistance to account for the heat flow from the liquid into the surroundings. The thermal resistance of the air is much larger than the thermal resistance of the

boundary layers. Figure 5 was plotted assuming no increase in heat flow through the boundary layer altered by the electric field (only one of the two boundary layers experiences an electric field). After the system has been running for a long time so that the temperatures have reached their steady-state values, the division of the heat input between the two sides of the plate depends on the total thermal resistance (boundary-layer thermal resistance plus air thermal resistance) on each side. Since the air thermal resistance is much larger than the boundary-layer thermal resistance, the change in boundary-layer resistance caused by the electric field causes essentially no change in the division of the input power between the two sides of the plate. However, when the system is first turned on the bulk of the liquid is at room temperature. At this time the division of the input heat power is determined by the ratio of the boundary-layer thermal resistances. The decrease in thermal resistance of one of the boundary layers caused by the voltage results in an increase in total heat flux through that boundary layer. Therefore initially the total heat flux through the boundary layer with the voltage applied is greater than it would have been with no voltage. This excess of heat flux over the no voltage value decreases in time until the heat flux is the same as it would have been for the no voltage case. (It should be noted that even though the heat flux is unchanged the Nusselt number is increased by a reduction in the temperature gradient.) Figure 5 does not take account of this excess heat flux. If it was accounted for the result would be to reduce significantly the scatter in data points for a single voltage. In Turnbull (1971) an increase in heat transfer was observed because of the d.c. electric field induced instability of the boundary layer. In the experiments reported here, however, the boundary layers were stable, allowing the theory developed in this paper to be applied.

An attempt to perform experiments with the electric field strongest at the top were unsuccessful because the non-heated electrode interfered with the boundary layer at the top and because the boundary layer became unstable at the top when a substantial voltage was applied.

This work was supported by the National Science Foundation under grant GK-14624.

REFERENCES

EDE, A. J. 1967 Advances in free convection. In *Advances in Heat Transfer* (ed. T. F. Irvine), vol. 4, p. 1. Academic.

SQUIRE, H. B. 1938 In *Modern Developments in Fluid Dynamics*, p. 641. Oxford University Press.

STRATTON, J. A. 1941 *Electromagnetic Theory*, p. 145. McGraw-Hill.

TURNBULL, R. J. 1969 Free convection from a heated vertical plate in a direct-current electric field. *Phys. Fluids*, **12**, 2255.

TURNBULL, R. J. 1970 Thermal diffusion effects on the electrohydrodynamic Rayleigh-Taylor bulk instability *Phys. Fluids*, **13**, 2615.

TURNBULL, R. J. 1971 Instability of a thermal boundary layer in a constant electric field. *J. Fluid Mech.* **47**, 231.